JAAS

Accepted Manuscript

This is an *Accepted Manuscript*, which has been through the Royal Society of Chemistry peer review process and has been accepted for publication.

Accepted Manuscripts are published online shortly after acceptance, before technical editing, formatting and proof reading. Using this free service, authors can make their results available to the community, in citable form, before we publish the edited article. We will replace this *Accepted Manuscript* with the edited and formatted *Advance Article* as soon as it is available.

You can find more information about *Accepted Manuscripts* in the Information for Authors.

Please note that technical editing may introduce minor changes to the text and/or graphics, which may alter content. The journal's standard Terms & Conditions and the Ethical guidelines still apply. In no event shall the Royal Society of Chemistry be held responsible for any errors or omissions in this *Accepted Manuscript* or any consequences arising from the use of any information it contains.

ROYAL SOCIETY OF CHEMISTRY

www.rsc.org/jaas

Optimization of a ^{48}Ca–^{43}Ca double-spike MC-TIMS method for measuring Ca isotope ratios ($\delta^{44/40}Ca$ and $\delta^{44/42}Ca$): limitations from filament reservoir mixing

Gregory O. Lehn[a]*, Andrew D. Jacobson[a]

[a] *Department of Earth and Planetary Sciences, Northwestern University, Technological Institute, 2145 Sheridan Road, Evanston, Illinois 60208, USA*

*Corresponding author gregorylehn@gmail.com, Tel: 1-847-467-2467.

Abstract

We used a Monte Carlo error model to optimize a ^{48}Ca–^{43}Ca double-spike technique for measuring Ca isotope ratios ($\delta^{44/40}Ca$ and $\delta^{44/42}Ca$) by Multi-Collector Thermal Ionization Mass Spectrometry (MC-TIMS). The model considers errors for counting statistics and Johnson noise, as well as changes in collector cup efficiency (drift). For a 20V ^{40}Ca ion-beam implemented in a three-hop, dynamic multi-collection routine, the model predicts that a wide range of $^{48}Ca/^{43}Ca$ and spike/sample ratios should yield internal precisions ($2\sigma_{SEM}$) of 0.015 – 0.020‰ for $\delta^{44/40}Ca$ and 0.025 – 0.030‰ for $\delta^{44/42}Ca$. Using a Thermo Fisher MC-TIMS (Triton), we tested $^{48}Ca/^{43}Ca$= 1.5 [$^{43}Ca/(^{48}Ca+^{43}Ca)$= 0.40 mol/mol] and spike/sample= 0.66 [$Ca_{dsp}/(Ca_{dsp}+Ca_{smp})$= 0.40 mol/mol] by repeatedly analyzing OSIL Atlantic seawater, NIST SRM 915a, NIST SRM 915b, USGS BHVO-1, and CaF_2 over 4 sessions spanning 1 month. While the measured internal precision generally agreed with model predictions, external reproducibility ($2\sigma_{SD}$) was much worse than expected. For the 81 measurements made, the average external reproducibility was 0.223‰ for $\delta^{44/40}Ca$ and 0.126‰ for $\delta^{44/42}Ca$. After processing raw data through the double-spike equations, nearly all fractionation-corrected ratios showed remnant fractionation patterns. Such patterns reflect deviation from ideal exponential mass-fractionation due to mixing of multiple, independently fractionating reservoirs on the filament. Additional model simulations, as well as comparison against $\delta^{44/40}Ca$ values determined with a ^{43}Ca–^{42}Ca double-spike, support the concept of an "average mass rule," which states that inaccuracies in fractionation-corrected data are greater for isotope ratios having an average mass further away from the average mass of the normalizing ratio. Until advancements are made to eliminate filament reservoir effects, ^{43}Ca–^{42}Ca and ^{46}Ca–^{43}Ca double-spikes should yield the most precise $\delta^{44/40}Ca$ and $\delta^{44/42}Ca$ values, respectively, when using MC-TIMS. Within the

limits of the ^{48}Ca–^{43}Ca double-spike technique, we observed no evidence for ^{40}Ca enrichments among the standards analyzed. Finally, we found that sample matrix effects do not influence the quality of Ca isotope measurements by MC-TIMS, and we tentatively propose that the external reproducibility determined from the repeated analysis of standards can represent the uncertainty of a single sample analysis.

1. Introduction:

Calcium (Ca) isotope measurements are relevant to diverse fields, including geochemistry, cosmochemistry, biology, medicine, archaeology, and anthropology [1-6]. Many studies employ "double-spike" techniques to correct for instrumental mass-fractionation when analyzing $^{40}Ca/^{44}Ca$ ratios by multi collector-thermal ionization mass spectrometry (MC-TIMS). The details and virtues of double-spiking have been extensively discussed in several publications[7-10]. The technique involves equilibrating a sample solution containing the element of interest with another solution containing a well-characterized mixture of two artificially enriched isotopes of the same element. Both the ratio of the two artificially enriched isotopes (the "double-spike" ratio) and the ratio of the double-spike to the sample (the "spike/sample" ratio) must be carefully optimized to minimize propagation of errors and achieve high precision results. Practically every double-spike combination, such as ^{48}Ca–^{43}Ca, ^{48}Ca–^{42}Ca, ^{46}Ca–^{43}Ca, and ^{43}Ca–^{42}Ca, has been implemented to measure $^{40}Ca/^{44}Ca$ ratios by MC-TIMS[11-15]. However, while different methods appear reasonably accurate, large differences in external reproducibility exist for reasons that are not entirely understood but appear to extend beyond simple mathematical optimization of the ratio defined above[9, 10]. Possible explanations for decreased precision include ion optical aberrations[13-15], sample matrix effects[10, 16], filament reservoir mixing[16-18], changes in collector cup efficiency (drift)[19, 20], and choice of the double-spike pair relative to the sample isotope ratio of interest[21]. These issues plague analysis of many isotope systems, but they are especially problematic for resolving the small abundance variations inherent to the Ca isotope system. To increase statistical confidence, it has become common practice to repeatedly analyze the same sample at the expense of efficiency and throughput. Moreover, in petrology[1, 22, 23], cosmochemistry[24], and some areas of biogeochemistry[15, 25, 26], it is desirable to determine whether

variation of the $^{40}Ca/^{44}Ca$ ratio reflects natural mass-fractionation, radiogenic ingrowth of ^{40}Ca from the decay of ^{40}K ($\tau_{1/2}$=1.277 x 10^9 yr), or some combination of the two. This question can be addressed by measuring a second isotope ratio, e.g., $^{42}Ca/^{44}Ca$, $^{40}Ca/^{42}Ca$, or $^{43}Ca/^{44}Ca$ [1, 22-25]. It is also possible to measure $^{40}Ca/^{44}Ca$ ratios with one double-spike pair but implement two sets of "true" ratios in the data reduction algorithms: the so-called "normal ratios"[11] and unspiked, internally normalized sample ratios[24, 27]. This latter approach requires two mass spectrometric runs.

Building on research by Holmden (2005) and Holmden and Bélanger (2010), Lehn et al. (2013) used a Monte Carlo error model to optimize a ^{43}Ca–^{42}Ca double-spike method for measuring $^{40}Ca/^{44}Ca$ ratios by MC-TIMS[14, 15, 20]. The model considers errors for counting statistics and Johnson noise, and it accounts for collector cup drift. Lehn et al. (2013) verified the model predictions by measuring four commonly analyzed Ca isotope standards (n=171) and demonstrated that $^{40}Ca/^{44}Ca$ ratios can be quantified with an internal precision ($2\sigma_{SEM}$) of ±0.024‰ and a long-term, external reproducibility ($2\sigma_{SD}$) of ±0.041‰, which represents a two-fold or better improvement over previously utilized methods[20]. The present study reports an effort where we used the Lehn et al. (2013) error model to optimize a ^{48}Ca–^{43}Ca double-spike MC-TIMS technique[20]. We selected this double-spike combination because it in theory allows simultaneous analysis of $^{40}Ca/^{44}Ca$ and $^{42}Ca/^{44}Ca$ ratios, thus offering potential to resolve mass-dependent fractionation from radiogenic ^{40}Ca enrichments in the context of a single run. (A ^{46}Ca-^{43}Ca double-spike offers the same potential, but we were unable to obtain a sufficiently pure ^{46}Ca spike.) In addition, other theoretical studies have suggested that a ^{48}Ca–^{43}Ca double-spike should yield more precise data than a ^{43}Ca–^{42}Ca double-spike[28], but in general, such assertions are challenging to verify because different studies employ slightly different models, assumptions, and measurement routines. Thus, in this study, we took care to reproduce as closely as possible the approach taken in Lehn et al. (2013) so that we could normalize variables and rigorously compare the two techniques[20].

2. Methods

2.1 Theoretical optimization of the ^{48}Ca-^{43}Ca double-spike using a Monte Carlo error model

We used the Monte Carlo error model presented in Lehn et al. (2013) to optimize a ^{48}Ca-^{43}Ca double-spike method allowing the simultaneous analysis of ^{40}Ca/^{44}Ca and ^{42}Ca/^{44}Ca ratios[20]. This section provides a brief overview of the model, and where appropriate, we present equations specific to the ^{48}Ca-^{43}Ca double-spike method. Following Eugster et al. (1969), we derived the following equations for the determination of ^{40}Ca/^{44}Ca and ^{42}Ca/^{44}Ca ratios using a ^{48}Ca-^{43}Ca double-spike:

$$\left(\frac{^{48}Ca}{^{43}Ca}\right)_{dsp} = \left(\frac{^{48}Ca}{^{43}Ca}\right)_{mix} + \left[\left(\frac{^{44}Ca}{^{43}Ca}\right)_{mix} - \left(\frac{^{44}Ca}{^{43}Ca}\right)^{tru}_{dsp}\right] \cdot \left[\frac{\left(\frac{^{48}Ca}{^{43}Ca}\right)_{mix} \cdot \left(\frac{^{43}Ca}{^{44}Ca}\right)^{tru}_{smp} - \left(\frac{^{48}Ca}{^{44}Ca}\right)^{tru}_{smp}}{1 - \left(\frac{^{44}Ca}{^{43}Ca}\right)_{mix} \cdot \left(\frac{^{43}Ca}{^{44}Ca}\right)^{tru}_{smp}}\right] \quad (1)$$

$$\left(\frac{^{XX}Ca}{^{44}Ca}\right)_{smp} = \frac{\left(\frac{^{XX}Ca}{^{43}Ca}\right)_{mix}}{\left(\frac{^{44}Ca}{^{43}Ca}\right)_{mix}} + \frac{\left[\frac{\left(\frac{^{XX}Ca}{^{43}Ca}\right)_{mix}}{\left(\frac{^{44}Ca}{^{43}Ca}\right)_{mix}} \cdot \left(\frac{^{44}Ca}{^{43}Ca}\right)^{tru}_{dsp} - \left(\frac{^{XX}Ca}{^{43}Ca}\right)^{tru}_{dsp}\right]}{\left[\left(\frac{^{44}Ca}{^{43}Ca}\right)_{mix} - \left(\frac{^{44}Ca}{^{43}Ca}\right)^{tru}_{dsp}\right]} \cdot \left[1 - \left(\frac{^{44}Ca}{^{43}Ca}\right)_{mix} \cdot \left(\frac{^{43}Ca}{^{44}Ca}\right)^{tru}_{smp}\right] \quad (2)$$

where *dsp*, *mix*, *tru*, and *smp* stand for double-spike, mixture, true, and sample, respectively[8]. In equation (2), the symbol *XX* refers to either ^{40}Ca or ^{42}Ca. Equations (1) and (2) are solved iteratively, as described in Lehn et al. (2013).

Double-spike compositions were simulated using abundance data for ISOFLEX ^{43}Ca- and ^{48}Ca-enriched $CaCO_3$ powders (www.isoflex.com; Table 1) according to the equation:

$$^{43}\mathrm{Ca}_{\mathrm{dsp}} = \frac{^{43}\mathrm{Ca}}{^{48}\mathrm{Ca} + {}^{43}\mathrm{Ca}} \ , \quad (3)$$

where the molar abundance of ^{43}Ca in the double-spike ($^{43}Ca_{dsp}$) ranges from 0 to 1. To calculate the composition of the spike-sample mixture, the simulated double-spike was combined with a sample having normal ratios[11] (Table 1) according to the equation:

$$\mathrm{p}_{\mathrm{dsp}} = \frac{\mathrm{Ca}_{\mathrm{dsp}}}{\mathrm{Ca}_{\mathrm{dsp}} + \mathrm{Ca}_{\mathrm{smp}}} \ , \quad (4)$$

where the molar proportion of Ca from the double-spike (p_{dsp}) ranges from 0 to 1. It follows from equations (3) and (4) that,

$$\left(\frac{^{48}\mathrm{Ca}}{^{43}\mathrm{Ca}}\right)_{\mathrm{dsp}} = \frac{1 - {}^{43}\mathrm{Ca}_{\mathrm{dsp}}}{{}^{43}\mathrm{Ca}_{\mathrm{dsp}}} \tag{5}$$

$$(\mathrm{dsp}/\mathrm{smp}) = \frac{\mathrm{p}_{\mathrm{dsp}}}{1 - \mathrm{p}_{\mathrm{dsp}}}\ , \tag{6}$$

where $(^{48}Ca/^{43}Ca)_{dsp}$ is the ^{48}Ca/^{43}Ca ratio of the double-spike and *dsp/smp* is the spike/sample ratio. An exponential law was used to simulate how mass-dependent fractionation changes the spike-sample mixture during ionization and measurement:

$$\left(\frac{^{a}\mathrm{Ca}}{^{b}\mathrm{Ca}}\right)_{\mathrm{frac}} = \left(\frac{^{a}\mathrm{Ca}}{^{b}\mathrm{Ca}}\right)_{\mathrm{ufrac}} \cdot \left(\frac{\mathrm{M_a}}{\mathrm{M_b}}\right)^{\beta}\ , \tag{7}$$

where *frac* and *ufrac* refer to fractionated and unfractionated, M_a and M_b are the exact atomic masses of Ca isotopes a and b, and β is the instrumental mass-fractionation factor. Both $^{43}Ca_{dsp}$ and p_{dsp} were stepped in 1% increments. We assumed a constant β of 0.5, based on laboratory observations. The model output is insensitive to the magnitude of β.

Because Ca isotopes have very different relative abundances and a wide mass spectrum, it is advantageous to implement a dynamic, multi-collection routine[14]. Consistent with Lehn et al. (2013), we adopted a three-hop duty cycle[20]. A hop refers to a change in the magnet field setting, and the three hops combine to yield one duty cycle. The first hop measures ^{40}Ca and ^{43}Ca in the L2 and H3 cups, respectively. The second hop measures ^{43}Ca and ^{48}Ca in the L4 and H4 cups, respectively. The third hop measures ^{42}Ca, ^{43}Ca, and ^{44}Ca in the L1, center (C), and H1 cups, respectively. For real measurements, ^{41}K is collected in L3 during the third hop to monitor the contribution of ^{40}K to the ^{40}Ca signal. The model does not consider isobaric interferences because real data are not collected unless ^{40}K is negligible. The ^{40}Ca/^{43}Ca (or ^{42}Ca/^{43}Ca), ^{48}Ca/^{43}Ca, and ^{44}Ca/^{43}Ca ratios implemented in the data reduction are taken directly from the first, second, and third hops. Unique integration times were considered for each hop, namely 4.194, 8.388, 16.772 and 33.542 s, but the sum of integration times for the three hops was limited to 45 s to avoid significant fractionation differences between the first and last hop during real measurements. We considered 30, 60, 90, and 120 duty cycles per run.

The ^{40}Ca ion-beam was set to 20V to be consistent with the approach taken in Lehn et al. (2013). Normally distributed errors were randomly assigned to the theoretically derived, instrumentally fractionated ratios[20]. Errors considered include those from counting statistics and Johnson noise[20, 29]. Ratios have variable errors because the errors depend on signal strength. Each pass through the three-hop duty cycle ultimately generates one $^{40}Ca/^{44}Ca$ ratio and one $^{42}Ca/^{44}Ca$ ratio. The model reduces hypothetical data for each duty cycle separately and averages multiple duty cycles to calculate a mean $^{40}Ca/^{44}Ca$ ratio and a mean $^{42}Ca/^{44}Ca$ ratio for the entire run. The internal precision is determined by doubling the standard error of the mean ratio ($2\sigma_{SEM}$). The model simulates each permutation 100 times and averages the data to arrive at the representative mean ratio and $2\sigma_{SEM}$. On a 100×100 grid of $^{43}Ca_{dsp}$ and p_{dsp} values, the combination of hops, integration times, and number of duty cycles yields >25,000,000 possible permutations for each ratio, $^{40}Ca/^{44}Ca$ and $^{42}Ca/^{44}Ca$. To limit the rate of collector damage and associated drift, we only considered methods delivering less than 6.5×10^{11} counts/sample to any collector[15, 20]. This number was derived from Holmden and Bélanger (2010), where drift was minimized for sessions involving 30 or fewer runs. With these constraints, we focused on values for $^{43}Ca_{dsp}$ and p_{dsp} yielding the optimal internal precision for $^{40}Ca/^{44}Ca$ and $^{42}Ca/^{44}Ca$ ratios, while minimizing analysis time and collector damage.

2.1 Ca Isotope Measurements

We verified the optimization by repeatedly measuring common standards, such as OSIL Atlantic Seawater (ASW), NIST SRM 915a, NIST SRM 915b, and USGS BHVO-1. The standards 915a and 915b are calcium carbonate powders, and BHVO-1 is a basaltic rock. We also analyzed Saskatchewan Isotope Lab gravimetric calcium fluoride (CaF_2). Measurements were made in the Radiogenic Isotope Clean Laboratory at Northwestern University using a Thermo Fisher Triton MC-TIMS. The optimal ^{48}Ca-^{43}Ca double-spike was prepared using ISOFLEX $^{48}CaCO_3$ and $^{43}CaCO_3$ powders (Table 1) and calibrated against the Saskatchewan Isotope Lab CaF_2 standard[14]. Table 1 provides the measured composition of the Northwestern University (NU) double-spike.

Spike-sample equilibration, purifications, filament loading, and the drift correction follow the protocols provided in Lehn et al. (2013)[20]. Table 2 summarizes instrumental parameters specific to the ^{48}Ca-^{43}Ca method. In brief, aliquots containing 50 µg of Ca were spiked and refluxed in acid-cleaned Teflon vials for several hours to ensure complete equilibration. Spiked aliquots of ASW, CaF_2, and BHVO-1 were purified by ion-exchange chromatography, using Teflon columns packed with Bio-Rad AG MP-50 cation exchange resin and ultrapure HCl eluents. The purified Ca solutions were dried and treated with 30% H_2O_2 to oxidize any organic compounds that might have leached from the resin. Spiked aliquots of 915a and 915b were not purified. All solutions were dried and treated with two drops of ultrapure HNO_3, to convert Ca to nitrate form. Single Ta filaments were outgassed under vacuum for 1.5 hours at 4800 mA, which is over 1500 mA higher than running conditions in the TIMS. Approximately 10-16 µg of Ca was loaded onto the outgassed filaments with 0.5 mg of 10% H_3PO_4 (Sigma-Aldrich *Trace*SELECT® Ultra H_3PO_4) and dried. The Ca was loaded between parafilm "dams" to prevent spreading on the surface of the filament. We also measured the ^{40}Ca/^{44}Ca ratio of BHVO-1 using the Lehn et al. (2013) ^{43}Ca-^{42}Ca double-spike method[20]. Unlike the ^{48}Ca-^{43}Ca double-spike method, the third hop of the ^{43}Ca-^{42}Ca double-spike method requires zoom optics. For all measurements, peak shapes were examined to confirm the absence of potential backscatter and reflections. All runs were checked for isobaric interferences from K, and occasionally, Ti and doubly-charged Sr[10]. No interferences were observed. We quantified our total procedural blank several times (n = 6) using isotope-dilution. The 500:1 sample-to-blank ratio is negligible. All ratios and their uncertainties are reported in delta notation, given in per mil, relative to OSIL Atlantic seawater (sw):

$$\delta^{44/XX}\mathrm{Ca}_{sw}\left(\text{in } ‰\right) = \left[\frac{\left(\frac{^{44}\mathrm{Ca}}{^{XX}\mathrm{Ca}}\right)_{sample}}{\left(\frac{^{44}\mathrm{Ca}}{^{XX}\mathrm{Ca}}\right)_{sw}} - 1\right] \cdot 1000\,, \qquad (8)$$

where *XX* refers to either ^{40}Ca or ^{42}Ca.

3. Results

Similar to optimization of the ^{43}Ca-^{42}Ca double-spike, the Monte Carlo simulations for the ^{48}Ca-^{43}Ca double-spike yielded a wide range of non-unique solutions[20]. To minimize analysis time and collector damage at a marginal expense to precision, we chose a method having 90 duty cycles with integration times of 4.194, 8.388, and 16.776 s for the first, second, and third hops, respectively. This method requires 2.5 hours/sample, including filament warm-up. Figures 1a and 1b show contour maps of the predicted internal precisions for $\delta^{44/40}$Ca and $\delta^{44/42}$Ca. Statistically identical internal precisions are possible for a wide range of double-spike and spike/sample ratios. Internal precision is more sensitive to p_{dsp} than $^{43}Ca_{dsp}$. We ultimately selected $^{43}Ca_{dsp}$= 0.40 and p_{dsp}= 0.40, as these values offer the best precision for both $\delta^{44/40}$Ca and $\delta^{44/42}$Ca during a single mass spectrometric run. For $\delta^{44/40}$Ca, the predicted internal precision ($2\sigma_{SEM}$) is ±0.015 – 0.020‰, and for $\delta^{44/42}$Ca, the predicted internal precision is 0.025 – 0.030‰.

Table 3 and Figure 2 summarize the standard measurements. For the 81 measurements made with the ^{48}Ca-^{43}Ca double-spike, the internal precision was more variable and on average, slightly higher than the model predictions. For $\delta^{44/40}$Ca, the measured internal precision ranged from 0.013 to 0.081‰, with an average of 0.025‰. For $\delta^{44/42}$Ca, the measured internal precision ranged from 0.020 to 0.093‰, with an average of 0.034‰. The external reproducibility ($2\sigma_{SD}$) for $\delta^{44/40}$Ca ranged from 0.201 to 0.253‰, with an average of 0.223‰, which is ~11 times higher than the average internal precision. The external reproducibility for $\delta^{44/42}$Ca ranged from 0.091 to 0.153‰, with an average of 0.126‰, which is ~4 times higher than internal precision. By comparison, the 6 measurements of BHVO-1 made with the ^{43}Ca-^{42}Ca double-spike yielded results consistent with findings reported in Lehn et al. (2013). The external reproducibility was 0.033‰, which is only ~1.5 times higher than the average internal precision of 0.023‰.

4. Discussion

4.1 Filament Reservoir Mixing

Poor external reproducibility for the ^{48}Ca-^{43}Ca method points to an additional source of error beyond counting statistics and Johnson noise. When examining uncorrected and fractionation-corrected

ratios within a given run, remnant fractionation patterns were observed for nearly all analyses. Some trends in the corrected ratios were linear, while others were curved or had multiple inflections. Figure 3 shows examples for one "good" run and two "bad" runs. For the good run, the uncorrected ratios show a linear fractionation trend that is eliminated after the fractionation correction and spike un-mixing. The bad runs show irregular fractionation trends that persist after the fractionation correction and spike un-mixing. Such patterns were not observed, or were minor, during development of the Lehn et al. (2013) method, and nor did we observe any remnant fractionation patterns during application of the ^{43}Ca-^{42}Ca double-spike in the present study. Because the ^{48}Ca-^{43}Ca and ^{43}Ca-^{42}Ca double-spike methods employed the same chemical separation, filament loading, filament heating, and drift correction protocols, we can eliminate these steps as possible sources of error. The patterns are consistent with deviation from ideal exponential mass-fractionation, caused by mixing of multiple, independently fractionating reservoirs on the filament[17, 18, 30]. Both double-spike methods experience this problem, but the effects are more evident and detrimental for the ^{48}Ca-^{43}Ca method according to the "average mass rule," which states that inaccuracies in fractionation-corrected data are greater for isotope ratios having an average mass further away from the average mass of the normalizing ratio[21, 31-33].

To examine this idea in more detail, we used the filament reservoir-mixing model presented in Fantle and Bullen (2009)[17] to generate theoretical, instrumentally fractionated Ca isotope ratios that were then reduced with the double-spike equations (Equations 1 and 2). The model simulates two pools of a spike-sample mixture that have the same starting composition but fractionate independently. Calcium isotope ratios in each pool are fractionated with the exponential law (Equation 7). However, β is now replaced with a time dependent value, β_t:

$$\beta_t = \beta_0 + \Delta\beta \cdot x\,, \tag{9}$$

where β_0 represents the starting fractionation factor based on modification during filament warm up and focusing, $\Delta\beta$ is rate of change for the fractionation factor as a function of duty cycle, and x is the duty cycle number. For each duty cycle, the percentage contribution of each pool to the total ion beam varies.

We considered two scenarios and a control summarized in Table 4. The scenarios were designed to simulate as closely as possible the filament mixing patterns shown in Figure 3. In the first scenario, one pool is the sole source of Ca ions for the first several duty cycles. Later, the other pool begins fractionating and delivers increasingly more Ca ions until the first pool completely decays. In the second scenario, the second pool begins fractionating during the first duty cycle and starts supplying Ca ions during the following duty cycle. The transition between the two pools occurs more slowly, such that they contribute equally by the end of the run. The control scenario simulates ideal fractionation from a single pool. The scope of our analysis includes the measurement of ^{40}Ca/^{44}Ca ratios with ^{48}Ca-^{43}Ca, ^{43}Ca-^{42}Ca, ^{48}Ca-^{42}Ca, and ^{46}Ca-^{43}Ca double-spikes and the measurement of ^{42}Ca/^{44}Ca ratios with ^{48}Ca-^{43}Ca and ^{46}Ca-^{43}Ca double-spikes.

Figure 4 illustrates the model output by plotting uncorrected ratios and simulated measurement errors (deviations) as a function of duty cycle number. Deviations, given in ppm/amu, are calculated as the difference between the true isotope ratio and the final output ratio after processing through the double-spike equations. Figures 4A and C demonstrate that simple reservoir mixing can reasonably simulate the actual uncorrected data provided in Figures 3C and E, while Figures 4B and D show that error magnitudes depend on the combination of double-spike and sample ratios. Analysis of ^{40}Ca/^{44}Ca ratios with a ^{43}Ca-^{42}Ca double-spike yields the lowest errors, followed by analysis of ^{42}Ca/^{44}Ca ratios with a ^{46}Ca-^{43}Ca double-spike. Analysis of ^{40}Ca/^{44}Ca ratios with a ^{46}Ca-^{43}Ca double-spike, ^{42}Ca/^{44}Ca ratios with a ^{48}Ca-^{43}Ca double-spike, and ^{40}Ca/^{44}Ca ratios with a ^{48}Ca-^{42}Ca double-spike all yield higher errors having a similar magnitude. Finally, analysis of ^{40}Ca/^{44}Ca ratios with a ^{48}Ca-^{43}Ca double-spike produces the highest errors.

To further examine these relationships, Figure 5 plots the average error for the various double-spike methods as a function of the average error for the measurement of ^{40}Ca/^{44}Ca ratios with a ^{43}Ca-^{42}Ca double-spike. The model scenarios define remarkably linear correlations. However, deeper consideration reveals that the correlations are insensitive to the details of the mixing model, such as the parameters in equation (9) or the percentage contribution of the two pools to the total ion beam. Other mixing simulations produce identical correlations. Rather, the results are consistent with predictions from the

average mass rule. For example, the average mass difference between the ^{43}Ca-^{42}Ca pair and the ^{40}Ca-^{44}Ca pair is 0.5 amu. The average mass difference between the ^{48}Ca-^{43}Ca pair and the ^{40}Ca-^{44}Ca pair is 3.5 amu. The ratio of 3.5 amu to 0.5 amu equals 7, which is effectively identical to the slope of 6.9 shown in Figure 5. In other words, the average mass rule predicts that errors attributable to filament reservoir mixing will always be roughly 7 times larger when analyzing ^{40}Ca/^{44}Ca ratios with a ^{48}Ca-^{43}Ca double-spike compared to a ^{43}Ca-^{42}Ca double-spike. Real measurements are consistent with this assertion. As reported in Section 3, analysis of ^{40}Ca/^{44}Ca ratios with the ^{48}Ca-^{43}Ca double-spike yields an external reproducibility of 0.22‰, whereas analysis of ^{40}Ca/^{44}Ca ratios with the ^{43}Ca-^{42}Ca double-spike yields an external reproducibility of 0.04‰[20]. The ratio of 0.22‰ to 0.04‰ equals 5.5. Most likely, the theoretical ratio (7) differs from the actual ratio (5.5) because the former only considers the error from filament reservoir mixing, whereas the latter also includes errors for counting statistics and Johnson noise, which differ between the two methods.

According to the average mass rule, errors for the analysis of ^{42}Ca/^{44}Ca ratios with a ^{46}Ca-^{43}Ca double-spike, ^{40}Ca/^{44}Ca ratios with a ^{46}Ca-^{43}Ca double-spike, ^{42}Ca/^{44}Ca ratios with a ^{48}Ca-^{43}Ca double-spike, and ^{40}Ca/^{44}Ca ratios with a ^{48}Ca-^{42}Ca double-spike will be approximately 3, 5, 5, and 6 times worse, respectively, than errors for the analysis of ^{40}Ca/^{44}Ca ratios with a ^{43}Ca-^{42}Ca double-spike. As shown in Figure 5, the corresponding slopes are 4.0, 5.4, 5.4, and 5.5. We note that the slopes provided in Figure 5 slightly differ from the predictions offered by the average mass rule (e.g., 6.9 versus 7, 4 versus 3, etc.). This is a second-order effect reflecting the double-spike and spike/sample ratios applied in the data reduction algorithm (see Table 4). Modestly adjusting the optimal ratios can entirely eliminate the discrepancies such that the average mass law predictions and mixing model slopes are identical.

Our findings surrounding the average mass rule lead to important conclusions and may offer new directions for improving the precision of Ca isotope measurements by MC-TIMS. It appears that efforts to optimize Ca isotope ratios by double-spike MC-TIMS should consider errors associated with filament reservoir mixing in addition to those for counting statistics and Johnson noise[20, 29, 34]. In fact, we suggest that the choice of the double-spike pair relative to the sample ratio of interest should be considered before

any attempt to optimize the double-spike and spike/sample ratios. While selecting a double-spike pair with a large mass difference may enable better quantification of the instrumental fractional factor[9], this seems secondary to constraints imposed by the average mass rule. As demonstrated here, filament reservoir mixing explains why the ^{48}Ca-^{43}Ca double-spike method consistently underperforms predictions from the optimization model. The present study and Lehn et al. (2013) provide compelling evidence that a ^{43}Ca-^{42}Ca double-spike offers the most precise analysis of ^{40}Ca/^{44}Ca ratios[20]. We go on to propose that a carefully optimized ^{46}Ca-^{43}Ca double-spike method should offer the most precise analysis of ^{42}Ca/^{44}Ca ratios, as the errors due to reservoir mixing will be smaller than those for the ^{48}Ca-^{43}Ca double-spike. However, these recommendations could change if techniques can be developed to limit reservoir mixing. Building on methods presented in Holmden and Bélanger (2010), Lehn et al. (2013) hypothesized that loading samples between parafilm dams would mitigate reservoir mixing on the filament[20], but the current study indicates that parafilm dams do not eliminate the problem. It is uncertain if reservoir mixing would be more prevalent without the dams, but we note that another study employing a ^{46}Ca-^{43}Ca double-spike found little difference with and without dams[35]. We load relatively large amounts of Ca on the filament (10 – 16 μg) to optimize counting statistics and because the ionization efficiency of Ca is notoriously poor. However, reservoir effects are likely more prevalent for large Ca pools. Using double and triple filament assemblies[25, 36-38] can enable smaller loads, improve ionization efficiency, slow the fractionation rate, and smooth fractionation patterns, all of which have potential to reduce reservoir mixing errors. Finally, selecting a double-spike pair with the same average mass as the sample ratio pair could in theory eliminate the effect entirely. Examples include using ^{46}Ca-^{40}Ca, ^{46}Ca-^{42}Ca, or ^{46}Ca-^{44}Ca double-spikes to measure ^{42}Ca/^{44}Ca, ^{40}Ca/^{48}Ca, and ^{42}Ca/^{48}Ca ratios, respectively. However, the natural abundances of Ca are highly unfavorable for such applications and introduce other limitations to high-precision measurements.

4.2 ^{40}Ca enrichments

Recent studies have highlighted potential problems with common Ca isotope standards. Controversy has developed around possible ^{40}Ca enrichments in 915a and/or seawater. Some studies have

reported mass-independent isotope enrichments in 915a[24, 27, 39]; others have interpreted small discrepancies in $^{40}Ca/^{44}Ca$ and $^{42}Ca/^{44}Ca$ measurements as a ^{40}Ca enrichment in seawater[16, 23]; and yet others have found no enrichment in either standard[1, 25, 26, 40]. While significant differences in external reproducibility exist, we find that the ^{43}Ca-^{42}Ca and ^{48}Ca-^{43}Ca double-spike methods yield the same $\delta^{44/40}Ca$ values for 915a and ASW[20], as well as the three other standards analyzed. As Figure 6 demonstrates, a plot of $\delta^{44/40}Ca$ versus $\delta^{44/42}Ca$ does not reveal significant ^{40}Ca enrichments.

4.3 Ca isotope error reporting

Consistent with the convention in radiogenic isotope geochemistry[41], we report external reproducibility as twice the standard deviation ($2\sigma_{SD}$) of repeated standard measurements. A recent study (Fantle and Tipper, 2014)[16] has argued that twice the standard error of the mean ($2\sigma_{SEM}$), based on multiple analyses of samples, better represents the external reproducibility of Ca isotope measurements because standards often have simple matrices that obviate the need for column chemistry and real samples have more complex matrices that can translate into outlier measurements, despite purification by ion-exchange chromatography. However, our data tentatively suggest that filament reservoir effects can fully explain outlier measurements. As shown in Table 3, matrix-rich standards purified by ion-exchange chromatography (ASW and BHVO-1), as well as matrix-poor standards purified by ion-exchange chromatography (CaF_2), can be measured within the same external reproducibility as matrix-poor standards loaded directly onto filaments (915a and 915b). This holds true for both the ^{43}Ca-^{42}Ca and ^{48}Ca-^{43}Ca double-spike techniques. These results indicate that the external reproducibility determined from the repeated analysis of standards can be assigned as the uncertainty for a single sample analysis. However, additional experiments specifically targeting matrix effects are required to confirm this hypothesis.

5. Conclusions

Building on previous research by Lehn et al. (2013), this study used a Monte Carlo error model to optimize a ^{48}Ca-^{43}Ca double-spike for measuring $\delta^{44/40}Ca$ and $\delta^{44/42}Ca$ values by MC-TIMS. We tested the optimization by repeatedly analyzing common Ca isotopes standards, such as OSIL Atlantic seawater, NIST SRM 915a, NIST SRM 915b, USGS BHVO-1, and CaF_2. For $\delta^{44/40}Ca$, the average external

reproducibility ($2\sigma_{SD}$) of ±0.223‰ was ~11 times higher than internal precision ($2\sigma_{SEM}$). For $\delta^{44/42}$Ca, the average external reproducibility of ±0.126‰ was ~4 times higher than internal precision. By comparison, $\delta^{44/40}$Ca values measured with a ^{43}Ca-^{42}Ca double-spike had an external reproducibility of ±0.04‰, which is only ~2 times higher than internal precision (Lehn et al, 2013). We attribute the poor performance of the ^{48}Ca-^{43}Ca double-spike to filament reservoir effects, which cause deviations from ideal exponential mass-fractionation during ionization. We employed a mixing model to examine why errors are either amplified or diminished for methods involving different combinations of double-spike and sample ratios. We found that the difference between the average mass of the double-spike pair and the sample ratio pair can be used to predict the extent of error magnification. These findings suggest that the "average mass rule" should be taken into consideration when selecting a Ca isotope double-spike method. Because the average mass difference between the ^{43}Ca-^{42}Ca pair and the ^{40}Ca-^{44}Ca pair is only 0.5 amu, the ^{43}Ca-^{42}Ca double-spike technique should provide the most precise analysis of $\delta^{44/40}$Ca values. Limiting the effects of filament reservoir mixing may further improve precision. Finally, we note that many of the problems that hamper the quality of Ca isotope measurements by MC-TIMS, such as collector cup drift[20, 35] and filament reservoir mixing[17], are not particularly unusual[18, 32, 33]. Carefully monitoring and accounting for these factors largely eliminates the need to repeatedly analyze the same sample, although it remains good practice to occasionally measure duplicates. With the ^{43}Ca-^{42}Ca double-spike method, our data suggest that the external reproducibility determined from the repeated measurement of standards could accurately represent the uncertainty assigned to a single sample measurement, but we note that additional experiments are required to fully test this idea.

6. Acknowledgements

The authors thank Chris Holmden for providing Saskatchewan Isotope Lab CaF_2 and for many thoughtful discussions that aided and improved this study. Insightful comments from four anonymous reviewers improved the manuscript. This work was supported by an Environmental Protection Agency STAR Fellowship awarded to G.O.L., as well as a Major Research Instrumentation Grant (EAR-0723151) and a

David and Lucile Packard Foundation Fellowship awarded to A.D.J. The study also benefited from NSF EAR-0643317 and NSF-0617585 awarded to A.D.J.

7. References

1. S. Huang, J. Farkaš and S. B. Jacobsen, *Earth and Planetary Science Letters*, 2010, **292**, 337-344.
2. L. M. Reynard, G. M. Henderson and R. E. M. Hedges, *Journal of Archaeological Science*, 2011, **38**, 657-664.
3. A. D. Melin, B. E. Crowley, S. T. Brown, P. V. Wheatley, G. L. Moritz, F. T. Yit Yu, H. Bernard, D. J. DePaolo, A. D. Jacobson and N. J. Dominy, *American journal of physical anthropology*, 2014, DOI: 10.1002/ajpa.22530.
4. N.-C. Chu, G. M. Henderson, N. S. Belshaw and R. E. M. Hedges, *Applied Geochemistry*, 2006, **21**, 1656-1667.
5. C. Holmden, K. Panchuk and S. C. Finney, *Geochimica Et Cosmochimica Acta*, 2012, **98**, 94-106.
6. C. Holmden, D. A. Papanastassiou, P. Blanchon and S. Evans, *Geochimica Et Cosmochimica Acta*, 2012, **83**, 179-194.
7. M. Dodson, *Geochimica et Cosmochimica Acta*, 1970, **34**, 1241-1244.
8. O. Eugster, F. Tera and G. J. Wasserburg, *J. Geophys. Res.*, 1969, **74**, 3897-3908.
9. D. J. DePaolo, *Reviews in mineralogy and geochemistry*, 2004, **55**, 255-288.
10. A. Heuser, A. Eisenhauer, N. Gussone, B. Bock, B. T. Hansen and T. F. Nagler, *International Journal of Mass Spectrometry*, 2002, **220**, 385-397.
11. W. A. Russell, D. A. Papanastassiou and T. A. Tombrello, *Geochimica et Cosmochimica Acta*, 1978, **42**, 1075-1090.
12. T. F. Nagler, A. Eisenhauer, A. Muller, C. Hemleben and J. Kramers, *Geochemistry Geophysics Geosystems*, 2000, **1**.
13. I. R. Fletcher, A. L. Maggi, K. J. R. Rosman and N. J. McNaughton, *International Journal of Mass Spectrometry and Ion Processes*, 1997, **163**, 1-17.
14. C. Holmden, *Measurement of δ44Ca Using a 43Ca-42Ca Double-spike TIMS*, Saskatchewan Geological Survey, 2005.
15. C. Holmden and N. Bélanger, *Geochimica et Cosmochimica Acta*, 2010, **74**, 995-1015.
16. M. S. Fantle and E. T. Tipper, *Earth-Science Reviews*, 2014, **129**, 148-177.
17. M. Fantle and T. Bullen, *Chemical Geology*, 2009, **258**, 50-64.
18. S. R. Hart and A. Zindler, *International Journal of Mass Spectrometry and Ion Processes*, 1989, **89**, 287-301.
19. R. S. Hindshaw, B. C. Reynolds, J. G. Wiederhold, R. Kretzschmar and B. Bourdon, *Geochimica et Cosmochimica Acta*, 2011, **75**, 106-118.
20. G. O. Lehn, A. D. Jacobson and C. Holmden, *International Journal of Mass Spectrometry*, 2013, **351**, 69-75.
21. K. Gopalan, D. Macdougall and C. Macisaac, *International Journal of Mass Spectrometry*, 2006, **248**, 9-16.
22. S. Huang, J. Farkaš and S. B. Jacobsen, *Geochimica et Cosmochimica Acta*, 2011, **75**, 4987-4997.
23. J.-S. Ryu, A. D. Jacobson, C. Holmden, C. Lundstrom and Z. Zhang, *Geochimica et Cosmochimica Acta*, 2011, **75**, 6004-6026.
24. J. I. Simon and D. J. DePaolo, *Earth and Planetary Science Letters*, 2010, **289**, 457-466.
25. J. Farkaš, A. Déjeant, M. Novák and S. B. Jacobsen, *Geochimica et Cosmochimica Acta*, 2011, **75**, 7031-7046.
26. G. Caro, D. A. Papanastassiou and G. J. Wasserburg, *Earth and Planetary Science Letters*, 2010, **296**, 124-132.
27. J. I. Simon, D. J. DePaolo and F. Moynier, *The Astrophysical Journal*, 2009, **702**, 707.

28. J. F. Rudge, B. C. Reynolds and B. Bourdon, *Chemical Geology*, 2009, **265**, 420-431.
29. S. G. John and J. F. Adkins, *Marine Chemistry*, 2010, **119**, 65-76.
30. D. Upadhyay, E. E. Scherer and K. Mezger, *Journal of Analytical Atomic Spectrometry*, 2008, **23**, 561.
31. G. J. Wasserburg, S. B. Jacousen, D. J. DePaolo, M. T. McCulloch and T. Wen, *Geochimica et Cosmochimica Acta*, 1981, **45**, 2311-2323.
32. D. Vance and M. Thirlwall, *Chemical Geology*, 2002, **185**, 227-240.
33. R. Andreasen and M. Sharma, *International Journal of Mass Spectrometry*, 2009, **285**, 49-57.
34. S. G. John, *Journal of Analytical Atomic Spectrometry*, 2012, **27**, 2123-2131.
35. R. S. Hindshaw, PhD, ETH, 2011.
36. L. C. Nielsen and D. J. DePaolo, *Geochimica et Cosmochimica Acta*, 2013, **118**, 276-294.
37. E. J. Catanzaro, *Journal of Geophysical Research*, 1967, **72**, 1325-1327.
38. L. Moore, E. Heald and J. Filliben, 1978.
39. M. Schiller, C. Paton and M. Bizzarro, *Journal of Analytical Atomic Spectrometry*, 2012, **27**, 38.
40. M. Amini, A. Eisenhauer, F. Böhm, C. Holmden, K. Kreissig, F. Hauff and K. P. Jochum, *Geostandards and Geoanalytical Research*, 2009, **33**, 231-247.
41. P. Deines, S. L. Goldstein, E. H. Oelkers, R. L. Rudnick and L. M. Walter, *Chemical Geology*, 2003, **202**, 1-4.

Table Captions

Table 1: Isotopic abundances of Ca normal, Ca single spikes, and Northwestern University (NU) double-spikes

Table 2: Method settings for Triton MC-TIMS

Table 3: Ca isotope results for 5 standards using the ^{48}Ca-^{43}Ca and ^{43}Ca-^{42}Ca double-spike techniques

Table 4: Input parameters for filament reservoir mixing model

Figure Captions

Figure 1: Contour plots of theoretical (A) $\delta^{44/40}$Ca and (B) $\delta^{44/42}$Ca internal precisions ($2\sigma_{SEM}$) using a ^{48}Ca-^{43}Ca double-spike. The model output reflects a 20 V ^{40}Ca beam and 90 duty cycles with integration times of 4.194, 8.388, and 16.766 s for hops 1, 2, and 3, respectively. The curves represent theoretical thresholds for collector damage (6.5 x 10^{11} counts/sample) as a function of $^{43}Ca_{dsp}$ and p_{dsp} for collectors L4, L1, C, H1, H3, and H4. The filled circle marks the optimal ^{48}Ca-^{43}Ca double-spike composition tested in this study ($^{43}Ca_{dsp}$ = 40% and p_{dsp} = 40%).

Figure 2: $\delta^{44/40}$Ca and $\delta^{44/42}$Ca values for ASW, 915a, 915b, CaF_2 and BHVO-1. Circles show data measured with the ^{48}Ca-^{43}Ca double-spike method. Diamonds show $\delta^{44/40}$Ca values for BHVO-1 measured with the ^{43}Ca-^{42}Ca double-spike method. The dotted lines denote average values. The gray areas display external reproducibility ($2\sigma_{SD}$).

Figure 3: Fractionation patterns observed in uncorrected and corrected data for 915b obtained with the ^{48}Ca-^{43}Ca double-spike method. Panels A and B show data with minimal fractionation patterns. Panels C – D and E – F provide different examples of filament reservoir effects. The dashed lines in Panels B, D, and F display the mean 915b value for this study (Table 3).

Figure 4: Uncorrected and corrected data from the filament reservoir mixing model. Panels A and B show data for scenario 1, and Panels C and D show data for scenario 2 (see Table 4). Mixing scenarios 1 and 2 were designed to simulate real data from Figure 3. Note that results for $\delta^{44/40}$Ca measured with a ^{48}Ca-^{42}Ca double-spike, $\delta^{44/40}$Ca measured with a ^{46}Ca-^{43}Ca double-spike, and $\delta^{44/42}$Ca measured with a ^{48}Ca-^{43}Ca double-spike overlap.

Figure 5: Summary of filament reservoir mixing model results. Errors for $\delta^{44/4X}$Ca measured with different double-spikes are plotted against errors for $\delta^{44/40}$Ca measured with a ^{43}Ca-^{42}Ca double-spike. Note that three sets of results overlap (see caption for Figure 4). The slopes demonstrate how errors propagate according to predictions from the average mass rule. Other parameters, such as the double-spike and spike/sample ratios, also influence the magnitude of errors, but to a lesser degree than the choice of the double-spike pair relative to the sample ratio of interest. See text.

Figure 6: $\delta^{44/42}$Ca versus $\delta^{44/40}$Ca for five standards analyzed with a ^{48}Ca-^{43}Ca double-spike. Error bars represent $2\sigma_{SEM}$ reported in Table 3. The solid line shows theoretical kinetic mass fractionation (slope = 0.488). The dashed line shows theoretical equilibrium mass fractionation (slope = 0.476). Both lines are

anchored to zero on the seawater scale, although this does not convey less uncertainty for ASW. Both lines provide an acceptable fit to the data within the uncertainties.

Table 1

Isotope	Ca normal [a]	$^{48}CaCO_3$ [b]	$^{43}CaCO_3$ [b]	^{48}Ca-^{43}Ca double-spike [c]	^{43}Ca-^{42}Ca double-spike [d]
^{40}Ca	0.9698	0.0272	0.0540	0.0396	0.0435
^{42}Ca	0.0064	0.0002	0.0018	0.0009	0.4678
^{43}Ca	0.0013	0.0001	0.90 ± 0.006	0.3626	0.4630
^{44}Ca	0.0206	0.0015	0.0444	0.0191	0.0256
^{46}Ca	0.0000	<0.0001	<0.0001	0.0002	0.0000
^{48}Ca	0.0018	0.971 ± 0.002	0.0008	0.5775	0.0002

a: Russell et al. (1978)
b: Isoflex.com
c: Measured in this study, see text
d: Lehn et al. (2013)

Table 2

Method Parameter	Setting
^{43}Ca abundance in ^{48}Ca-^{43}Ca double-spike	$^{43}Ca_{dsp}$=$^{43}Ca/(^{48}Ca + ^{43}Ca)$= 0.40 mol/mol
Double-spike ratio	$(^{48}Ca/^{43}Ca)_{dsp}$=(1-$^{43}Ca_{dsp}$)/$^{43}Ca_{dsp}$= 1.5 mol/mol
Proportion of spike Ca in spike -sample mixture	p_{dsp}= $Ca_{dsp}/(Ca_{dsp}+ Ca_{smp})$=0.40 mol/mol
Spike-sample ratio	dsp/smp= $p_{dsp}/(1-p_{dsp})$ = 0.66 mol/mol
Filament assembly	Single Ta (0.002" h x 0.030" w)
Ca load	10 - 16 µg
^{40}Ca ion beam intensity	20 V
Accelerating voltage	10 kV
Resistors	10^{11} Ω
Source Vacuum	< 1 x 10^{-7} mbar
Analyzer Vacuum	< 6 x 10^{-9} mbar
Hop 1	^{40}Ca (L2), ^{43}Ca (H3), 4.194 s
Hop 2	^{43}Ca (L4), ^{48}Ca (H4), 8.338 s
Hop 3	^{41}K (L3), ^{42}Ca (L1), ^{43}Ca (axial), ^{44}Ca (H1), 16.776 s
Idle time	4 s after each hop
Duty cycles	90
Blocks	9 (1 block= 10 duty cycles)
Gain Calibration	Every 3 samples
Focus	Warm-up and every 4 blocks
Peak center	Warm-up and every 4 blocks
Baseline	Before each block, defocused, 30 cycles at 1.05 s/cycle
Amplifier rotation	After each block
Total analysis time/ sample	2.5 h

Table 3

	^{48}Ca-^{43}Ca double-spike							^{43}Ca-^{42}Ca double-spike			
Standard Name	$\delta^{44/40}Ca_{sw}$	$2\sigma_{SD}$	$2\sigma_{SEM}$	$\delta^{44/42}Ca_{sw}$	$2\sigma_{SD}$	$2\sigma_{SEM}$	n	$\delta^{44/40}Ca_{sw}$	$2\sigma_{SD}$	$2\sigma_{SEM}$	n
OSIL Atlantic SW	0.000	0.224	0.047	0.000	0.135	0.028	23	-	-	-	-
915b	-1.144	0.234	0.054	-0.585	0.136	0.031	19	-	-	-	-
915a	-1.839	0.264	0.054	-0.930	0.153	0.033	22	-	-	-	-
CaF_2	-1.398	0.201	0.061	-0.666	0.091	0.028	11	-	-	-	-
BHVO-1	-1.061	0.203	0.083	-0.494	0.115	0.047	6	-1.085	0.033	0.013	6

Table 4

Double-spike methods		
^{48}Ca-^{43}Ca	$^{43}Ca_{dsp}$= 0.40 and p_{dsp}= 0.40 (This Study)	
^{48}Ca-^{42}Ca	$^{42}Ca_{dsp}$= 0.3964 and p_{dsp}= 0.1424 (Rudge et al., 2009)	
^{46}Ca-^{43}Ca	$^{43}Ca_{dsp}$= 0.4898 and p_{dsp}= 0.2239 (Rudge et al., 2009)	
^{43}Ca-^{42}Ca	$^{42}Ca_{dsp}$= 0.50 and p_{dsp}= 0.25 (Lehn et al., 2013)	
Scenario #1	Pool 1	Pool 2
Starting Parameters		
Fractionation begins	x=1	x=11
β_0	0.235	0
$\Delta\beta$	0.0025	0.0025
Percentage Contribution to ion beam (%)		
Duty Cycle		
1 to 10	100	0
11 to 76	=Previous value − 1.5%	=100 − Pool 1
77 to 90	0	100
Scenario #2	Pool 1	Pool 2
Starting Parameters		
Fractionation begins	x=1	x=1
β_0	0.300	0
$\Delta\beta$	0.0025	0.0025
Percentage Contribution to ion beam (%)		
Duty Cycle		
1	100	0
2 to 90	=Previous value − 0.6%	=100 − Pool 1
Control	Pool 1	Pool 2
Starting Parameters		
Fractionation begins	x=1	n/a
β_0	0.500	n/a
$\Delta\beta$	0.0025	n/a
Percentage Contribution to ion beam (%)		
Duty Cycle		
1 to 90	100	0

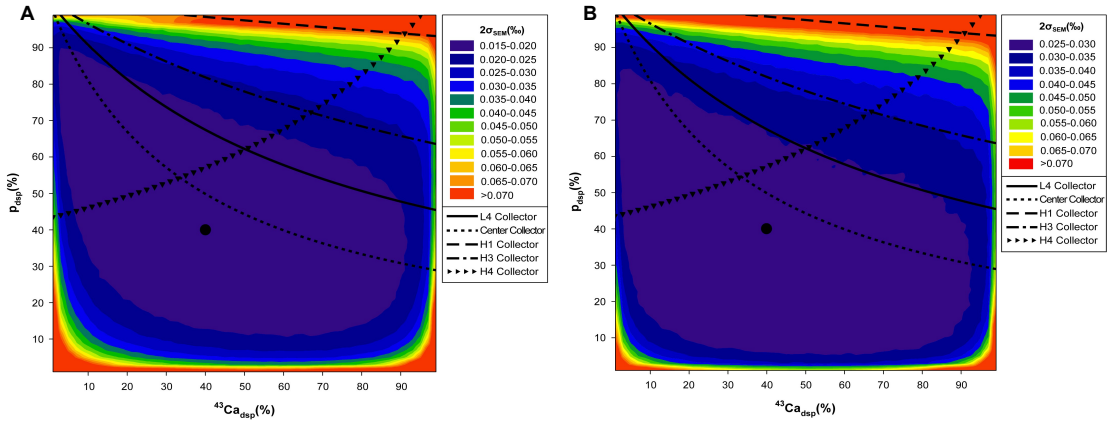

Figure 1

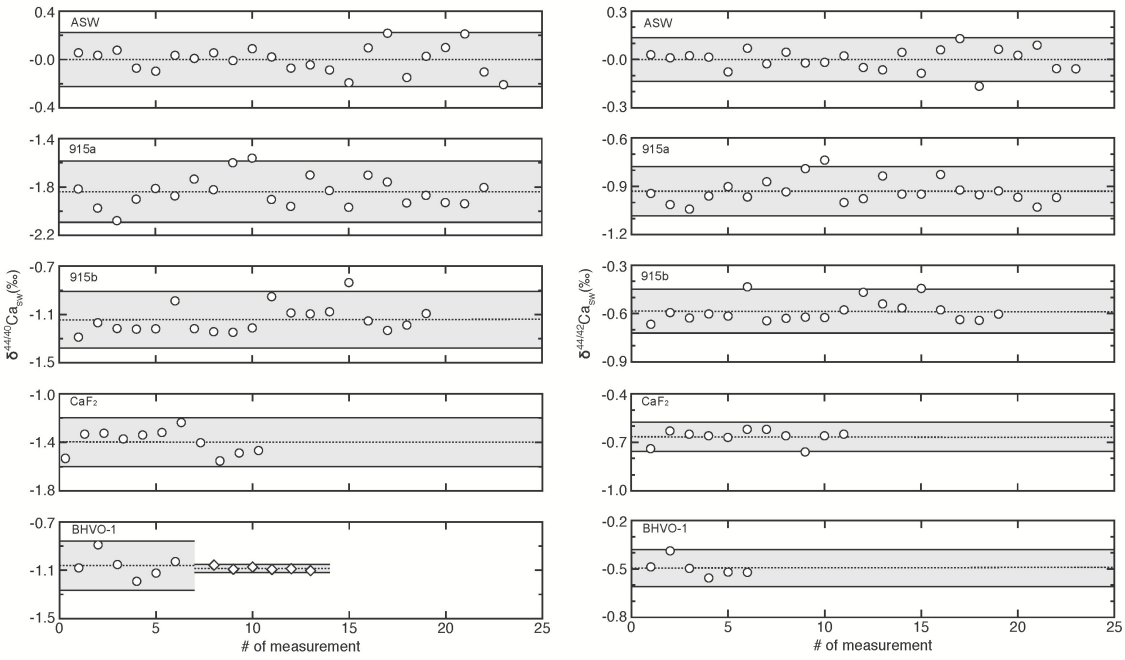

Figure 2

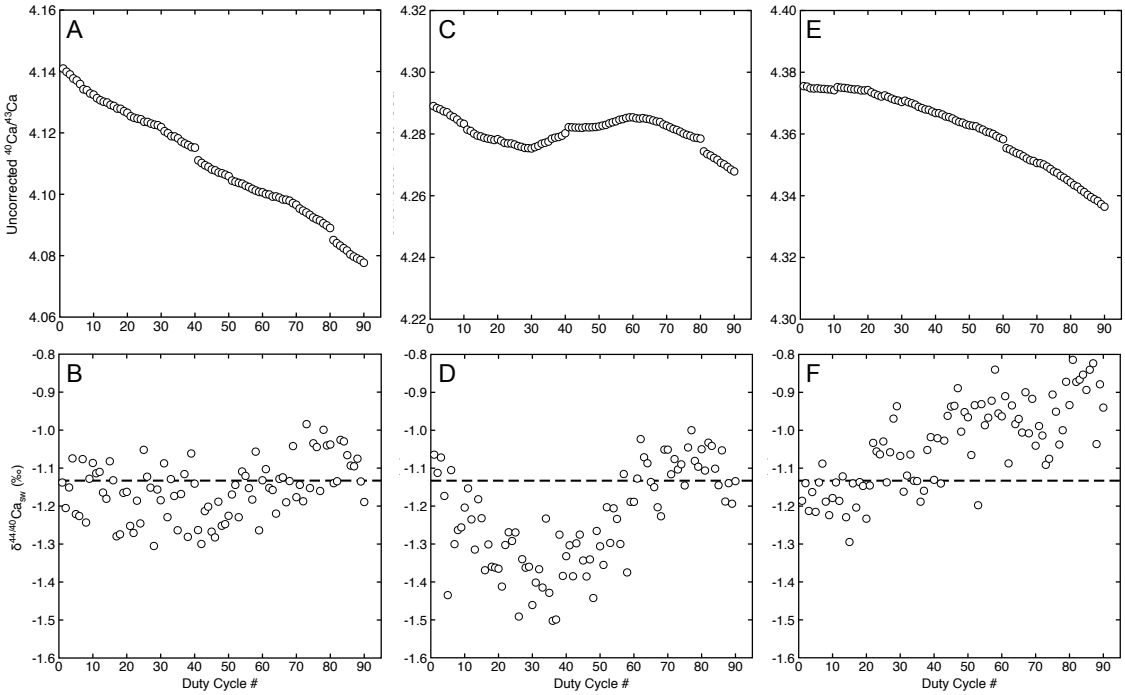

Figure 3

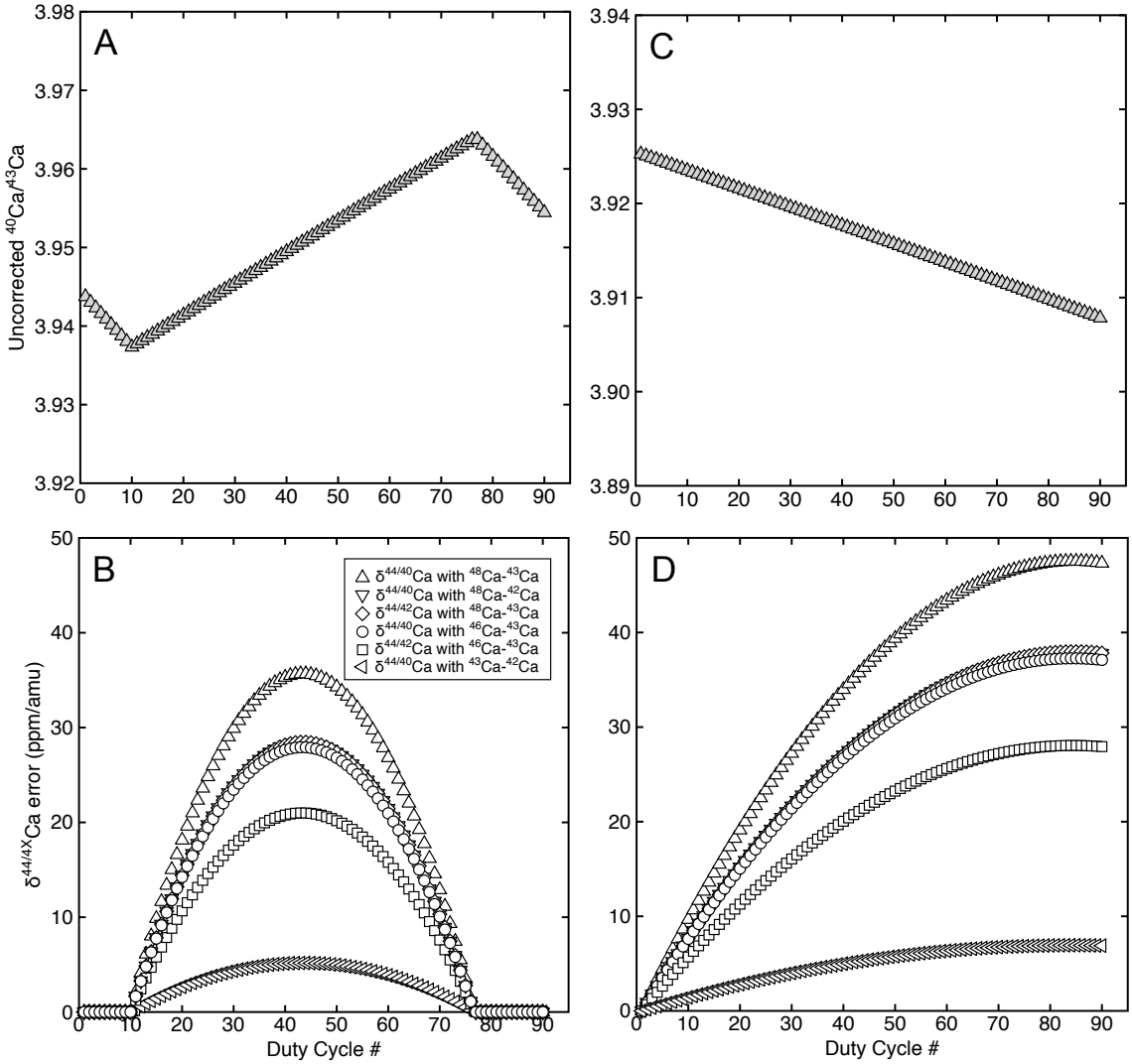

Figure 4

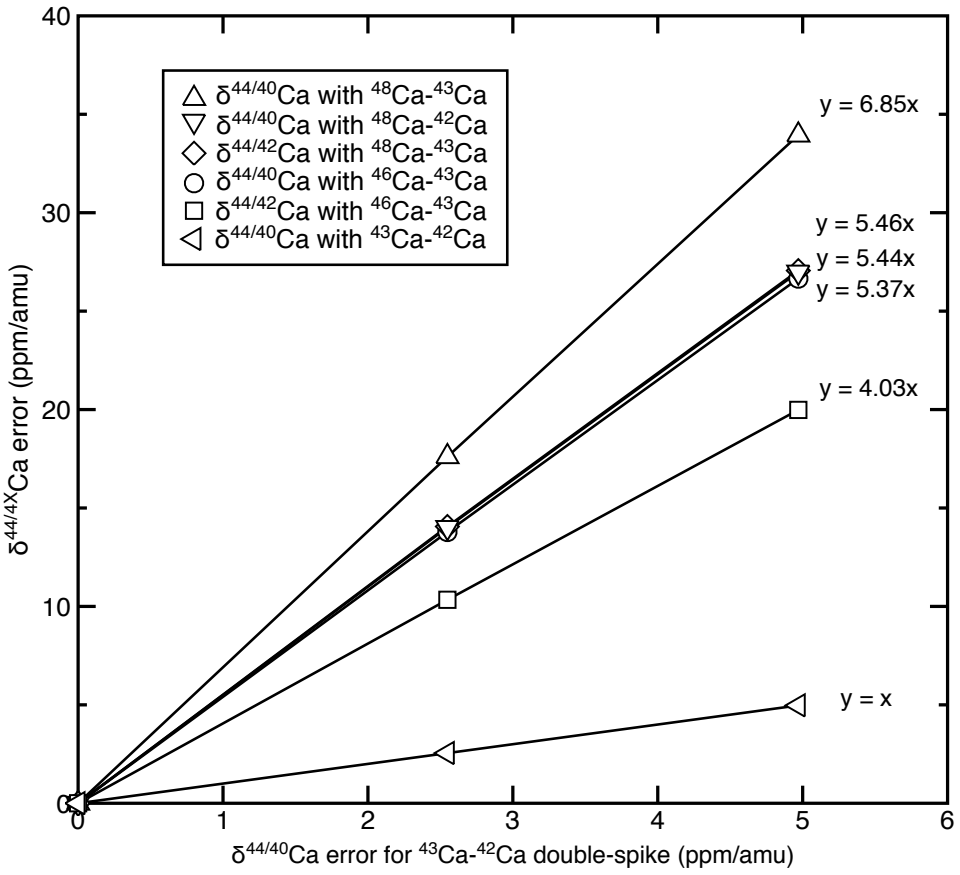

Figure 5

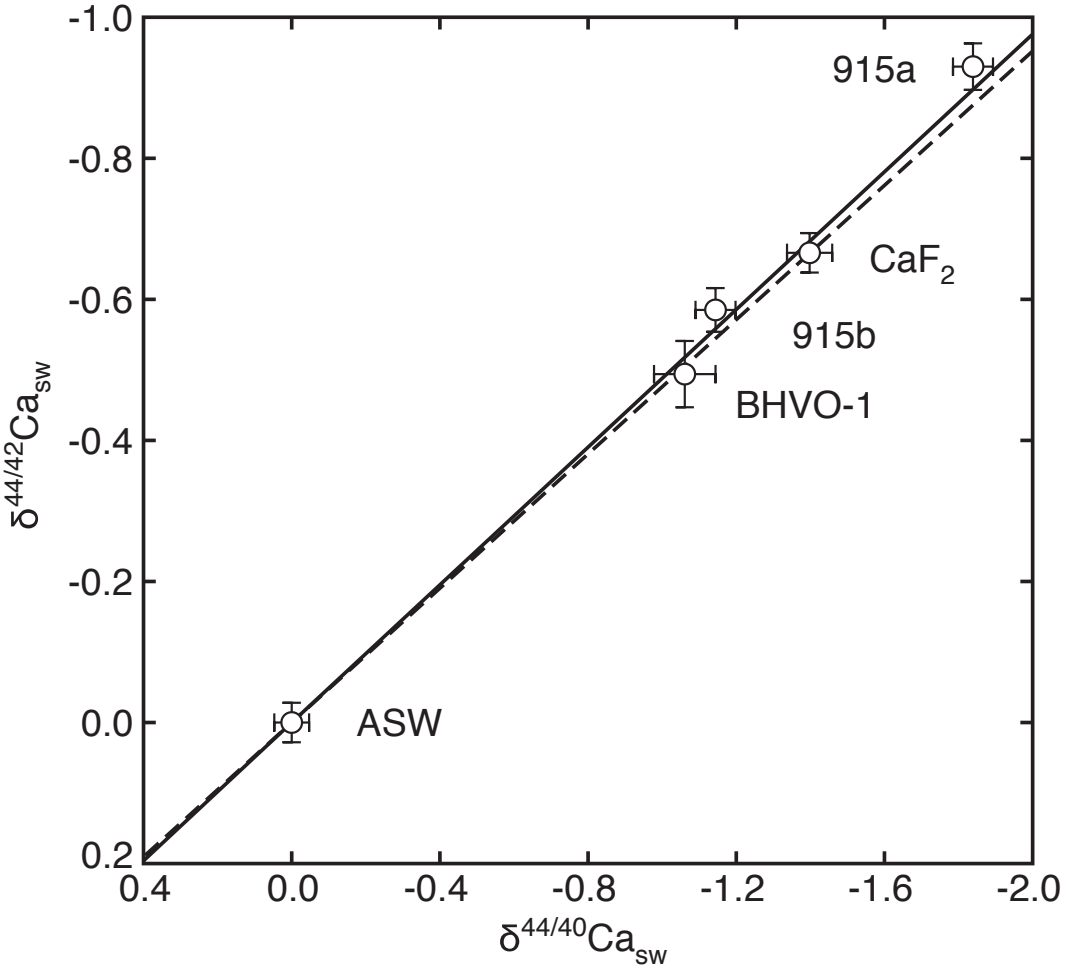

Figure 6